SRP-35 A NEWLY IDENTIFIED PROTEIN OF THE SKELETAL MUSCLE SARCOPLASMIC RETICULUM IS A RETINOL DEHYDROGENASE.

[1,2]Susan Treves, [1]Raphael Thurnheer, [2]Barbara Mosca, [1]Mirko Vukcevic [2]Leda Bergamelli, [2]Rebecca Voltan, [3]Vitus Oberhauser, [4]Michel Ronjat, [5]Laszlo Csernoch, [5]Peter Szentesi and [1,2]Francesco Zorzato

[1]Departments of Anesthesia and of Biomedicine, Basel University Hospital, Hebelstrasse 20, 4031 Basel, Switzerland; [2]Department of Experimental and Diagnostic Medicine, General Pathology section, University of Ferrara, Via Borsari 46, 44100 Ferrara, Italy; [3]Albert-Ludwigs-Universität Freiburg Institut für Biologie I (Zoologie), Hauptstrasse 1, 79104 Freiburg, Germany; [4]Unité Inserm U836, Université Joseph Fourier, Grenoble Institute of Neuroscience, Site Santé, 38700 La Tronche, France; [5]Department of Physiology, University of Debrecen, Nagyerdei krt. 98, 4012 Debrecen, Hungary

Running title: SRP-35 a retinol dehydrogenase, is expressed in muscle

Address correspondence to: Prof. F. Zorzato, Department of Experimental and Diagnostic Medicine, University of Ferrara, Via Borsari 46, 44100 Ferrara, Italy. TEL +39-0532-455-356; FAX +39-0532-2653502; E-mail zor@unife.it

In the present report we provide evidence that SRP-35, a protein we identified in rabbit skeletal muscle sarcoplasmic reticulum, is an all-*trans* retinol dehydrogenase. Analysis of the primary structure and tryptic digestion revealed that its NH_2-terminal encompasses a short hydrophobic sequence bound to the sarcoplasmic reticulum membrane, while its COOH-terminal catalytic domain faces the myoplasm. SRP-35 is also expressed in liver and adipocytes where it appears in the post-microsomal supernatant, however in skeletal muscle SRP-35 is enriched in the longitudinal sarcoplasmic reticulum. Sequence comparison predicts that SRP-35 is a short-chain dehydrogenase/reductase belonging to the DHRS 7C subfamily. Retinol is the substrate of SRP-35 since its transient over-expression leads to an increased production of all-*trans* retinaldehyde. Transfection of C_2C_{12} myotubes with a fusion protein encoding SRP-35-EYFP causes a decrease of the maximal Ca^{2+} released via ryanodine receptor activation induced by KCl or 4-chloro-m-chresol. The latter result could be mimicked by the addition of retinoic acid to the C_2C_{12} cell tissue culture medium, a treatment which caused a significant reduction of RyR1 expression. We propose that in skeletal muscle SRP-35 is involved in the generation of all-*trans* retinaldehyde and may play an important role in the generation of intracellular signals linking Ca^{2+} release (i.e. muscle activity) to metabolism.

Introduction

The skeletal muscle sarcoplasmic reticulum (SR) is an intracellular membrane compartment highly specialized in calcium homeostasis. Structurally it can be subdivided into two membrane portions: the terminal cisternae facing the transverse tubules, and the longitudinal sarcoplasmic reticulum (LSR) that connects two terminal cisternae [1]. Depolarization of the plasma membrane causes the Ca^{2+} stored in the SR to be released, leading to muscle contraction by a process known as excitation-contraction coupling [2,3]; Ca^{2+} is then pumped back into the SR via sarco(endo)plasmc reticulum Ca^{2+} ATPases (SERCAs) which are located on the terminal cisternae and LSR, leading to muscle relaxation [4-6]. These highly

coordinated events occur within milliseconds thanks to the spatial organization of the membrane compartments carrying the different proteins involved in sensing plasma membrane depolarization, Ca^{2+} release and Ca^{2+} uptake [7]. Indeed, excitation-contraction coupling occurs at the triad a structure made up of the transverse tubules (which are invaginations of the plasma membrane), carrying the voltage sensing dyhydropyridine receptor (DHPR), and two terminal cisternae carrying the ryanodine receptor (RyR) Ca^{2+} release channel [8,9]. Although these two Ca^{2+} channels are the basic unit underlying excitation-contraction coupling, they nevertheless function in coordination with a number of accessory proteins and enzymes involved in maintaining the architecture and optimal function of the calcium release unit. Because of their potential roles in regulating excitation-contraction coupling and since they may be targets of mutations causing neuromuscular disorders, several laboratories have focused their research on identifying novel proteins present on these specialized intracellular membrane compartments and a number of minor components including mitsugumins, junctophilins, junctate, JP-45 and SRP27 have recently been characterized [for recent reviews see 10, 11].

In the present study, using a proteomic approach we identified a 35 kDa protein in skeletal muscle SR which we called SRP-35, for sarcoplasmic reticulum protein of 35 kDa. Sequence motif comparison indicates that this protein belongs to the DHRS7C short chain dehydrogenase (SDR) subfamily [12] and is likely to catalyse the conversion of all-*trans* retinol to retinaldehyde by reducing the cofactor NAD^+ to NADH [13]. SDRs are ubiquitously expressed and constitute a large protein family involved in the reduction of a variety of substrates, among which, retinol, the precursor of retinoic acid [14]. In vertebrates the effectors of RA signalling belong to the nuclear receptor family that are divided into two subgroups: the nuclear retinoic-acid receptors, (RARα/ß/γ) and the retinoid-X receptors (RXRα/ß/γ) [15-18]. Upon RA binding to RAR, the receptors undergo hetero-dimerization with RXRs and translocate into the nucleus, where they bind to target DNA sequences known as retinoic-acid response elements promoting the transcription of several genes, including some involved in growth, development, differentiation, cytokine production and metabolism [14,19]. Interestingly, treatment of mice with all-*trans* RA reduces body weight, adipose tissue content and promotes skeletal muscle fatty acid oxidation [20]. Thus SRP-35 may be part of a signalling pathway linking muscle activity and metabolism; indeed this polypeptide is enriched in tissues involved in fatty acid metabolism, notably liver, adipose tissue, kidney and skeletal muscle. Interestingly in the latter tissue it is enriched in the longitudinal sarcoplasmic reticulum where a number of glycolytic enzymes such as pyruvate kinase, aldolase, enolase and glyceraldehyde 3-phosphate dehydrogenase have also been found to compartmentalize [21]. Since SRP-35 oxidizes all-*trans* retinol (ROL) to all-*trans* retinaldehyde (RAL) at a site directly involved in Ca^{2+} homeostasis, we hypothesize that SRP-35 might have a dual function: (i) reduce NAD^+ linked to lactic acid generation. The NADH would in turn down-regulate Ca^{2+} release by affecting the redox equilibrium adjacent to RyR1 (the skeletal muscle isoform of the RyR); (ii) regulate skeletal muscle gene transcription via the retinoic acid receptor pathway.

Experimental procedures

Materials

Anti-calregulin and anti-calnexin antibodies, peroxidase-conjugated protein A, Trypsin-EDTA, DMEM, MEM plus Earls salts, L-Glutamine, Pennicillin/Streptomycin, horse serum, foetal bovine serum, Deoxyribonuclease I, Alexa Fluor 488 chicken anti-rabbit IgG and Alexa Fluor 568 donkey anti-mouse IgG were from Invitrogen. All-*trans* retinol and all-*trans* retinaldehyde, protein-A Sepharose, ESCORT IV, peroxidase conjugated protein G, peroxidase conjugated anti-mouse IgG and rabbit anti-DHRS7C Abs were from Sigma-

Aldrich. Mouse mAb anti-RyR1 (MA3-925) and anti-SERCA (MA3-910) were from Thermo Scientific. The pGEX-5X-3 plasmid and HiTrap Blue Sepharose were from GE Healthcare. The UNI-ZAP XR cDNA library, pEYFP-C1, pEGFP-C1 plasmids were from Clontech. Goat anti-DHPRα1.1 was from Santa Cruz. Anti-albumin antibodies were from Bethyl laboratories (Montgomery, TX., U.S.A). Oxy-Blot protein oxidation detection kit was from Millipore. Nitrocellulose membrane was from Schleicher & Schuell BioScience GmbH. Protein Molecular Weight markers and the Protein Assay kit were from Biorad. NAD^+, NADH, $NADP^+$, FuGene 6, anti-proteases, Taq polymerase were from Roche Diagnostics. The High Capacity cDNA Reverse transcription kit and fast SYBR green master mix were from Applied Biosystems (Forster City, CA, U.S.A.) Fura-2 acetoxymethylester was from Calbiochem. Tri-Reagent (Molecular Research Center Inc.). PCR primers were from Microsynth A.G. (Balgach, Switzerland). Paraffin-embedded mouse skeletal muscle sections were from Ciochain Institute Inc. (BioCat, Heidelberg, Germany). All other chemicals were reagent of highest available grade. Mice were bred in house and rabbits (NZW) were purchased from Charles Rivers Laboratories. All procedures were performed in accordance with the stipulations of the Helsinki Declarations for care and use of laboratory animals.

Methods

Protein sequencing: proteins present in the terminal cisternae and junctional face membrane fractions were separated on a 10% SDS PAG prepared under ultraclean conditions and allowed to polymerise at room temperature for 72 hours; the gel was stained with Coomassie Brilliant Blue R250 (0.1% CBB R250 in 50% MetOH, 0.1% Ac Acid) and destained overnight at 4°C in 1% acetic acid, 50% Methanol; the 35 kDa band was cut out with a clean scalpel blade and the SDS and CBB were removed by slicing the gel finely in 40% n-propanol, washing and vortexing the sample and changing the solution many times. After the last n-propanol wash, the gel was resuspended in a solution containing 0.2 M NH_4HCO_3/40% acetonitrile and washed with this solution 5 times. After the final wash, excess liquid was removed and the gel fragments dried in a speedvac. The sample was then rehydrated in 0.1 M NH_4CO_3/trypsin (sequencing grade, 25 ng/µl) and incubated at 37°C overnight. The supernatant was then collected and transferred to a clean tube; the pellet was treated with a solution made up by 80% acetonitrile/0.1% trifluoroacetic acid to extract remaining peptides. The two supernantants were combined and dried in a speedvac and then subjected to Mass Spec analysis using a Q-TOF (Micromass, Manchester, UK) mass spectrometer [22].

SRP-35 cDNA cloning- Total RNA was isolated from mouse skeletal muscles using Tri-Reagent following the instructions provided by the manufacturer. Total RNA was converted to cDNA as previously described [23] and primers were designed based on the peptide sequence obtained from trypsin digestion of rabbit SRP-35. These primers (5'-GGAGAGCCTCTACGCTGCCT-3'and 5'-ACGCCAACTACTTTGGACCCA -3' for forward and reverse reactions, respectively) were used to amplify a sequence from mouse skeletal muscle cDNA; a band of approximately 220 bp was obtained using the following amplification conditions: 1 cycle 95°C 5 min followed by 35 cycles annealing (55°C, 30 sec), extension (72°C, 45 sec), denaturation (95°C, 45 sec), followed by a 5 min extension cycle at 72°C. The PCR-amplified cDNA was then used as a probe to screen a mouse skeletal muscle UNI-ZAP XR cDNA library as previously described [23]. A clone of 960 bp, containing the entire ORF was pulled out and sequenced (Microsynth AG, Balgach, Switzerland). The coding sequence of SRP-35 was subcloned into the pGEX-5X-3 bacterial expression plasmid and into pEGFPC1 and pEYFPC1 for expression in mammalian cells.

Cell culture and transfection- C_2C_{12} cells were cultured in growth medium (DMEM+ glutamax+ high glucose (4.5g/l), 20% foetal calf serum, 200mM L-glutamine, penicillin/ streptomycin) and maintained below confluence. For differentiation into myotubes, cells were

allowed to reach 70% confluence then the medium was switched to differentiation medium (DMEM+ Glutamax+ high glucose, 5% horse serum, 200mM L-glutamine, penicillin/ streptomycin), until cells had visibly fused into myotubes (about 5 days). Transfection of C_2C_{12} cells was carried out using FuGene 6 at a ratio of 1.5 µl FuGene per µg plasmid DNA per ml culture media. Cells were transfected on day 1 and 3 following switch to differentiation medium and harvested on day 4 post differentiation. In some experiments C_2C_{12} were incubated for 4 days with retinoic acid (5 µM) during differentiation.

HEK 293 cells were cultured and transfected with the pEGFPC1 and pEGFPC1-SRP-35-plasmids using ESCORT IV as previously described [24].

Subcellular fractionation, trypsin digestion and fluorescence analysis- Total microsomes from different mouse tissues (heart, lung, brain, kidney, skeletal muscle, liver, spleen, stomach, intestine), total homogenates prepared form mouse tissues and from isolated fast (EDL) and slow (soleus) fibres, and skeletal muscle SR subfractions enriched in plasma membrane, terminal cisternae and longitudinal SR were prepared as described [1,23,24]. In order to determine if SRP-35 is an integral membrane protein, mouse skeletal muscle SR vesicles were treated with Na_2CO_3/KCl, as previously described [25]. Fifteen micrograms of mouse skeletal muscle SR were digested with increasing concentrations of trypsin, for 2 minutes at room temperature. The reaction was blocked by the addition of trypsin inhibitor; samples were then loaded onto a 12.5% SDS PAG, blotted onto nitrocellulose and probed with the indicated antibodies. Localization of GFP-tagged recombinant proteins in transfected C_2C_{12} cells was performed 48 hours after transfection. Briefly, myotubes were fixed with 3.7% paraformaldehyde (in PBS), mounted in glycerol medium and observed under fluorescent light (excitation 480 nm, emission 510 nm) with an inverted fluorescent microscope (Axiovert S100 TV/Carl Zeiss GmbH) equipped with a 20x water-immersion FLUAR objective (0.75 numerical aperture) attached to a Cascade 128+ CCD camera (Photometrics).

Polyclonal antibody production, Western blotting and confocal microscopy- Polyclonal antibodies raised against the recombinant GST-SRP-35 fusion protein were obtained by immunizing rabbits and the IgG fraction was purified as previously described [25]. Alternatively, commercial rabbit anti-DHRS7C were tested on blotted proteins and indirect immuno-enzymatic staining was carried out as previously described [25]. Confocal microscopy was performed on paraffin embedded mouse skeletal muscle tissue sections; briefly, sections were re-hydrated by incubating sequentially in Xylene (2 times, 2 min), 100% ethanol (2 times, 30 sec), 95% and 80% ethanol (1 time, 30 sec) followed by H_20 (3 times, 3 min) and equilibration in PBS; membranes were permeabilized for 30 min at room temperature with a solution containing 0.5% Triton X-100, 2% horse serum and 1% BSA; slides were then incubated with the primary antibody (rabbit anti-DHRS7C and mouse anti-SERCA mAb diluted in 0.01% Triton X-100, 1% BSA, 2% horse serum in PBS overnight at 4°C, followed by 4 washes 15 min each with PBS and incubation for 40 minutes at room temperature with Alexa Fluor-488 chicken anti-rabbit IgG and Alexa Fluor-568 donkey anti-mouse IgG diluted in 0.01% Triton X-100, 1% BSA, 2% horse serum in PBS. Slides were mounted and fluorescence observed by confocal microscopy using a Leica DM1400 confocal microscope equipped with a 100x HCX APO TIRF objective (1.47 NA).

Affinity Chromatography- In order to determine whether SRP-35 is a dinucleotide binding protein, we used the affinity column HiTrap Blue Sepharose; the ligand Cibacron Blue F3G-A shows structural similarities to NAD(H) enabling proteins strongly binding to this cofactor to attach to the resin [26]. Total SR vesicles (1 mg/ml) were solubilised for 30 min at 4° C in a solution containing 10 mM Tris-HCl pH 8.0, 1% DDM, 1 M NaCl. The solubilised SR membrane proteins were diluted 10 times with a solution containing Tris-HCl pH 8.0, 1 M NaCl and then incubated with Cibacron Blue F3G-A Sepharose previously equilibrated with

10 mM Tris-HCl pH 8.0, 0.1 % DDM, 1M NaCl. The resin was washed with 10 bed volumes of buffer containing 10 mM Tris-HCl pH 8.0, 0.1 % DDM, 1M NaCl and proteins were eluted by adding 1 mM NADH. In order to verify if some SRP-35 was still bound to the resin, 100 µl of laemmli loading buffer were added to the Cibacron Blue F3G-A Sepharose, after 5 min of incubation, samples were centrifuged and 30 µl of supernatant were loaded on the gel.

Ca^{2+} release and KCl-dose response curves- glass cover slip grown, transfected (with pEYFPC1 or pEYFPC1-SRP-35) and differentiated C_2C_{12} cells were loaded with the ratiometric Ca^{2+} indicator fura-2-AM (5µM) in Krebs-Ringer for 30 minutes at 37°C. YFP-positive cells were first identified using a 40x Plan-Neofluar objective (NA 1.3) and filter set N°44 (Carl Zeiss MicroImaging, Inc.; BP 475/40, FT 500, BP 530/50) as previously described [24]. Transfected cells were then analysed for their response to pharmacological activation with KCl or 4-chloro-m-cresol, or for the status of the intracellular Ca^{2+} stores by treating the cells with 5 µM ionomycin plus 1 µM thapsigargin in Krebs Ringer containing no added Ca^{2+} and 0.5 mM EGTA, by monitoring the changes in fura-2 fluorescence [27]. Images were acquired with a Cascade 128+ CCD camera and analysed using the Metamorph imaging software 7.7.0.0. Generation of dose response curves and statistical analysis were performed using Windows GraphPad Prism v.4.00 (GraphPad Software Inc.). For some experiments myotubes were treated with retinoic acid (5 µM) for 4 days, loaded with fura-2 and analysed for their calcium response to KCl and 4-chloro-m-cresol as indicated above.

Retinol/retinal enzymatic assays- HEK293 cells were transfected with pEYFPC1 or pEYFPC1-SRP-35 and 24 hours post transfection either all-*trans* retinol (10 µM) was added to the cell medium for 6 h, or all-*trans* retinaldehyde (5 µM) was added to the cell medium for 3 h. After incubation, the cells were washed twice with PBS and the medium replaced with 1 ml 100% methanol and 1 ml 2 M hydroxylamine pH 6.7. Cells were subsequently scraped off from the tissue culture flask, homogenized in a glass potter and after a 10 min incubation at room temperature, the homogenate was stored at –80°C until used.

For retinol quantification, all solutions were made diluting a stock solution of all-*trans* retinol or all-*trans* retinaldehyde prepared in 100% ethanol, to an aqueous solution containing 10 µM BSA (when all-*trans* retinol was added) or 5 µM BSA (when all-*trans* retinaldehyde was added) followed by sonication for 10 min. The final concentration of ethanol did not exceed 1% v/v. This procedure guarantees a more soluble and stable retinoid substrate solution [28]. One volume of 2 M hydroxylamine pH 6.7 and one volume of 100% methanol were added to quench the reaction and to stabilize the retinoids. Retinoid extraction from 500 µl of the homogenates was optimized by adding acetone (1 volume) as a phase mixing agent followed by three times extraction with petrol ether (0.6 volumes). The organic solvent was evaporated under a stream of nitrogen and the retinoid pellet was dissolved in 100 µl of HPLC mobile phase (99.5 hexane: 0.5 ethanol), and injected into the HPLC. The relative amounts of retinaldehyde and retinol are expressed as percentages (the amount of a retinoid specie divided by the total amount of all retinoids present).

Real time PCR- Total RNA was extracted from C_2C_{12} cells and treated with Deoxyribonuclease I as previously described [29]. After reverse transcription using 1000 ng of RNA, cDNA was amplified by quantitative real-time PCR using SYBR Green technology as previously described [29] and the following primers: RyR1 (forward 5′-GCACACAGTCGTATGTACCTG-3′ and reverse 5′-CCTCCCCTGTTGCGTCTTC-3′), SRP-35 (forward 5`-CCCTGGAGCTTGACAAAAAGA`-3′ and reverse 5′-GTTCACTAACACAATCTGGCCT-3′) $Ca_v1.1$ (forward 5`-TCAGCATCGTGGAATGGAAAC-3′ and reverse 5′-GTTCAGAGTGTTGTTGTCATCCT-3′). Gene expression was normalized using self-TATA box binding protein (TBP) as

reference and the following primers: forward, 5'- GCCATAAGGCATCATTGGAC-3' and reverse, 5'-AACAACAGCCTGCCACCTTA-3'.

Software and statistical analysis- Blast alignments were performed on the NCBI web site using BLAST 2.2.8. Multiple sequence alignments were performed using the Clustal W algorithm available from the Swiss node of the European Molecular Biology Network. Statistical analysis was performed using the Student's *t* test for two populations. Values were considered significant when $P<0.05$.

RESULTS

Primary structure of SRP-35- The skeletal muscle sarcoplasmic reticulum junctional face membrane is enriched in proteins playing a major role in Ca^{2+} homeostasis. One of the aims of the research of our and other laboratories is to identify all the protein constituents of this membrane fraction [10,11,30]. Results obtained by electronspray mass spectrometry analysis revealed the presence of a novel polypeptide with an approximate molecular mass of 35 kDa in the sarcoplasmic reticulum. Based on the amino acid sequence obtained from two peptides of the 35 kDa rabbit skeletal muscle protein (Fig.1 light grey boxes), primers were designed and used to amplify by RT-PCR (from mouse skeletal muscle mRNA) a cDNA sequence of approximately 960 nucleotides, whose primary sequence matched that of a hypothetical mouse protein present in the NCBI database (see Fig. 1). The predicted primary sequence of SRP-35 encompasses (i) the peptide sequences obtained from the rabbit skeletal muscle protein from which primers were designed (light grey boxes); (ii) an amino terminal hydrophobic sequence (dark grey box) which may be a signal sequence or a trans-membrane domain; (iii) an NAD(P)(H)-binding and catalytic site (underlined sequence); the bold letters indicate perfectly conserved residues within the NAD(P)(H)-binding and catalytic sites. Blast search analysis of the human genome revealed that the human homologue of the rabbit protein maps to human chromosome 17p13.1 (access number NM_00110557) and specifically to the DRS7C_human locus (dehydrogenase/reductase SDR family member 7C or SDR32C2); polymorphisms/mutations have so far not been associated with any human genetic disorder. Figure 1 also shows that SRP-35 is conserved among mammals (87-95% identity with the mouse sequence); however not all vertebrates express the 7C member of the SDR family of dehydrogenase/reductases and in fact BLAST analysis revealed that the gene encoding SDR7C is less conserved but present in the genomes of Xenopus (73% identity), Drosophila (38% identity) and Zebrafish (58% identity).

Tissue distribution, subcellular localization and membrane topology of SRP-35- In order to gain information concerning its physiological function, we analysed the tissue distribution of SRP-35 by western blot using two anti-SRP35 polyclonal antibodies (with similar results), one raised against the GST-SRP-35 fusion protein and the other, a commercially available one, raised against the putative DHRS7C gene product. Figure 2A shows that an immunoreactive band of approximately 35 kDa is present in the total homogenate of different mouse tissues, including adipose tissue, liver and skeletal muscle. Interestingly, in liver SRP-35 is not present in the microsomal fraction but remains in the 100,000 *g* supernatant (figure 2B), while in skeletal muscle it is highly enriched in the total SR fraction (figure 2C) and undetectable in the post microsomal supernatant (result not shown). In all other tissues tested the 35 kDa immunoreactive protein is undetectable in the microsomal fraction. These results indicate that in muscle, SRP-35 may interact with macromolecules that are exclusively present in skeletal muscle. Because we were interested in the functional role of SRP-35 in skeletal muscle, all subsequent experiments were performed on this tissue.

The subcellular distribution of SRP-35 was analysed: (i) in isolated fractions of the sarco(endo)plasmic reticulum, (ii) by monitoring the expression of GFP-tagged SRP-35 in C_2C_{12} myotubes and (iii) by confocal microscopy on mature mouse skeletal muscle

longitudinal sections. Figure 2D shows that SRP-35 is enriched in the skeletal muscle fraction corresponding to the longitudinal SR. Quantitative immunoblot analysis revealed that the immunopositive band corresponding to SRP-35 is enriched 6 fold (5.97± 0.2, mean± SEM;n= 6) in longitudinal sarcoplasmic reticulum compared to total muscle homogenate (Supplementary Fig. 1). These results are compatible with the distribution of fluorescence in C_2C_{12} myotubes transfected with GFP-tagged SRP-35 (figure 2F). As shown, transfection of C_2C_{12} cells with pEGFP results in an even cytoplasmic distribution of GFP-fluorescence, whereas when cells expressed the SRP-35-GFP fusion protein, the resulting punctuated fluorescence is compatible with the localization of SRP-35 in a membrane bound organelles. High-resolution confocal analysis on longitudinal sections of mouse skeletal muscle, shows a cross-striated distribution of endogenous SRP-35 with a centre to centre distance between the bands of approximately 1.5 µm. This fluorescent pattern partially overlaps with that of the SERCA pump (see Supplementary Figure 2), indicating a common subcellular distribution. A similar expression pattern was observed after *in vivo* transfection of FDB fibres with the SRP-35-EGFP construct (not shown). Interestingly and as shown in figure 2H slow twitch fibres contain significantly less SRP-35 than fast twitch fibres (the mean ±SEM, n=6 percentage intensity of the immunopositive band in western blots from soleus was 69.7±5.6% of that from EDL $P<0.0001$).

Based on its deduced primary sequence, the amino-terminal of this protein encompasses a hydrophobic peptide of 24 residues, which could be a signal sequence or may form a trans-membrane alpha-helical segment. To establish whether in skeletal muscle SRP-35 is an integral membrane protein we (i) extracted SR vesicles with KCl/Na_2CO_3 and (ii) performed trypsin digestion followed by western blot analysis. Treatment of mouse total SR membrane fraction with 0.6M KCl, a procedure used to separate loosely bound proteins from the membrane of microsomal vesicles, did not dissociate SRP-35 from the SR vesicles (Fig.3A left panel). The failure to extract SRP-35 with high-ionic strength wash might be due to the localization of SRP-35 in the lumen of the SR vesicles similarly to calsequestrin (Fig. 3A right panel) or it might result from its integral association to the SR membrane. To discriminate between these possibilities we performed an alkaline extraction of the SR fraction with 100 mM Na_2CO_3. As expected, calsequestrin (fig. 3B right panel), an intra-lumenal SR protein, was found in the Na_2CO_3 solubilized fraction. In contrast, SRP-35 was still associated with the insoluble membrane fraction (fig. 3B left panel), as was calnexin, a 90 kDa integral membrane protein of the endoplasmic reticulum (fig. 3B central panel). We further tested under what conditions SRP-35 could be solubilized, by treating SR vesicles with different detergents (CHAPS, DHPC and DDM) under high ionic conditions. As shown, extraction with 1% CHAPS was not efficient, whereas the treatment of SR vesicles with 1% DHPC or DDM in the presence of 1M NaCl was equally efficient at solubilizing SRP-35 (figure 3C). Finally, the topological orientation of SRP-35 was assessed by proteolysis of SR vesicles with increasing concentrations of trypsin. Under our experimental conditions, the immunoreactivity of SRP-35 decreased with increasing trypsing concentration even at very low trypsin concentrations (30 and 150 ng) while at these concentrations the immunoreactivity of calregulin, which is a luminal SR protein and thus not exposed to trypsin, was unaffected (figure 3 panels D). These results indicate that the majority of the SRP-35 polypeptide, including its epitope(s), protrudes from the SR vesicles and is exposed towards the myoplasm and only a small portion is bound to the SR membrane.

SRP-35 binds the dinucleotide NAD(H) and has catalytic activity- In silico comparison analysis of the deduced amino-acid sequence of SRP-35 revealed that it shares homology with proteins belonging to the short-chain dehydrogenases/reductases family. In order to determine whether it indeed binds dinucleotides, the affinity column HiTrap Blue Sepharose was used; the ligand Cibacron Blue F3G-A shows structural similarities to NAD(H) enabling

proteins strongly binding to this cofactor to attach to the resin [26]. Solubilized SR proteins were incubated with HiTrap Blue Sepahrose, the resin was extensively washed and bound proteins were eluted with 1 M NaCl plus NADH. The fraction(s) enriched in SRP-35 were identified by immunostaining with anti-SRP-35 antibodies. Figure 4 shows a representative result; the left panels of figure 4A and B are Ponceau-Red stained membranes while the right panels are the same blots stained (A) with anti-SRP-35 antibodies and (B) with anti-calsequestrin antibodies as control. An immunoreactive band corresponding to SRP-35 is present in the total SR (lane 1), in the solubilized SR fraction (lane 3) and in the NADH eluted fraction (lane 6). Not all SRP-35 was eluted with NADH as demonstrated by the presence of an immunoreactive band of 35 kDa in an aliquot of the Cibacron Blue F3G-A resin (lane 7). On the other hand, when the same experiment was performed by following the distribution of calsequestrin, a major SR protein which should not bind to Cibacron Blue F3G-A, its immunoreactivity is present in the total SR but not in the NADH eluate nor bound to the resin.

Since SRP-35 shares homology with the catalytic domains of classical SDR family members that convert, among others, retinol substrates to retinaldehyde derivatives, concomitantly reducing NAD, we set up an assay to validate the enzymatic activity of SRP-35 by verifying if its over-expression affects the amount of all-*trans* retinol (ROL) converted to all-*trans* retinaldehyde (RAL). As an experimental setup we chose an '*in situ*' whole cell assay in which transiently transfected cells (HEK293 cells or C_2C_{12} myotubes) were incubated with all-*trans* retinol or all-*trans* retinaldehyde and the amount of product formed was compared to that obtained in cells transiently transfected with the empty pEYFP plasmid. Panels C and D of figure 4 show original HPLC chromatograms obtained from lipid extracts of YFP and SRP-35- YFP transfected HEK293 cells, panels E and F show the cumulative results obtained by pooling data from three independent transfection experiments and normalized for the relative amount of all-*trans* retinaldehyde-oxim (peaks 2 and 5) and retinol (peak N° 4) divided by the total amount of peaks 1 through 5, defined as 100% (the total amount of all intracellular retinoids present in the lipid extracts). As shown, HEK293 cells over-expressing SRP-35 generate a significantly larger proportion of all-*trans* retinaldehyde (RAL; sum of peaks 2 and 5) compared to YFP transfected controls (fig. 4E). Interestingly, the reaction appears to preferentially proceed in the forward oxidative reaction since no change in the relative amount of all-*trans* retinol (ROL) was obtained in SRP-35 over-expressing cells (fig. 4F). Similar results were obtained in C_2C_{12} transfected myotubes (results not shown). In addition, 13-cis retinol was sometimes detected in the SRP-35-transfected HEK293 cells (peak 3), but may be an artefactual change of all-*trans*-retinol due to extraction procedure. We also verified if SRP-35 over-expression affects the overall redox status of cells by performing Oxy-Blot analysis on total extracts of GFP and SRP-35-GFP transfected HEK293 cells; as shown in Supplementary figure 3 cells transfected with the SRP-35 fusion protein exhibited a significant increase in the quantity of oxidatively modified proteins, confirming that SRP-35 is indeed involved in redox reactions.

Effect of SRP-35 over-expression on excitation-contraction coupling- SRP-35 is located within a subcellular membrane devoted to the regulation of the $[Ca^{2+}]$, thus we investigated if its over-expression affects Ca^{2+} homeostasis. C_2C_{12} mytotubes were transfected with the SRP-35-EYFP or with the empty pEYFP vector, loaded with fura-2 and individually stimulated with different concentrations of either KCl (mimicking depolarization) or 4-chloro-m-cresol (inducing direct activation of the RyR1). As shown in figure 5 over-expression of SRP-35 affected neither the resting $[Ca^{2+}]$ (fig. C) nor the EC_{50} for KCl (26.2 ±0.8 and 27.6± 1.8 mM for YFP and SRP-35-YFP over-expressing cells, respectively; fig. 5A) and 4-chloro-m-cresol (340.6±32.6 and 306.7±16.9 μM, for YFP and SRP-35-YFP over-expressing cells, respectively; fig. 5B) induced Ca^{2+} release; however, it significantly

decreased by approximately 40% the peak Ca^{2+} release induced by maximal stimulatory concentrations of KCl (fig.5D; $P<0.05$) and 4-chloro-m-cresol (fig. 5E; $P<0.008$). This decrease in peak Ca^{2+} release was not due to depletion of intracellular stores since the peak Ca^{2+} transients elicited by a treatment aimed depleting intracellular stores (5 μM ionomycine + 1 μM thapsigargin in 0.5 mM EGTA) were not significantly different (Δ fluorescence ratios were 0.251±0.041 and 0.205±0.048; $P=0.479$ in YFP and SRP-35-YFP expressing cells). Interestingly, addition of retinoic acid to C_2C_{12} during myotube differentiation mimicked the effect of SRP-35 over-expression by causing a significant decrease in the peak Ca^{2+} induced by KCl (fig. 5D; $P<0.01$) and 4-chloro-m-cresol (fig. 5E; $P<0.008$). The reduced Ca^{2+} release could be due to allosteric regulation by products deriving from the enzymatic activity of SRP-35 such as NADH and/or to alterations of the level of expression of the proteins involved in excitation-contraction coupling. The latter event may result from the effect of retinoic acid generated from the retinaldehyde produced by SRP-35. In order to investigate this, we performed Real Time PCR on mRNA extracted from C_2C_{12} myotubes treated in culture with 5 μM retinoic acid. We chose this approach to avoid the variability linked to the efficiency of transient transfections of C_2C_{12} cells. Figure 5F shows that retinoic acid treatment of C_2C_{12} myotubes induces a 2.5 fold induction in the level of expression of SRP-35; no affect was observed on the expression level of the alfa 1.1 subunit of the voltage sensing DHPR (fig.5G) but, interestingly, it caused a significant reduction (fig.5H; $P<0.025$) in the expression level of the mRNA encoding RyR1. This decrease in the RyR1 transcript was paralleled by a decrease in the content of the RyR1 protein as confirmed by western blot analysis (Supplementary figure 4). The extent of decrease of the mRNA level is similar to the extent of decrease of Ca^{2+} release observed after pharmacological activation of the RyR1 and most likely results from changes in the protein level of the RyR1 induced by retinoic acid production after 6 days of SRP-35 over-expression.

DISCUSSION

The skeletal muscle sarcoplasmic reticulum is an organelle specialized in regulating calcium homeostasis and identifying all its protein components constitutes a major step towards the elucidation of the regulation of calcium under normal and pathological conditions. In the present report we identified SRP-35 and show that this novel component of the skeletal muscle SR belongs to the short-chain dehydrogenase/reductase protein family, an enzyme whose activity may link calcium homeostasis to activation of metabolism.

The enzyme superfamily of short chain dehydrogenases consits of more than 46'000 family members which are ubiquitously expressed and whose transcripts have been found in virtually all genomes investigated [12, 31,32]. In the presence of specific co-factors they dehydrogenate numerous substrates including sterols, 3-hydroxysterols, alcohols, retinols, sugars, aromatic compounds and xenobiotics [33] thus playing critical roles in lipid, amino acid and carbohydrate metabolism; they also regulate many physiological processes by sensing the redox status in metabolism and transcription [13]. Although SDR share little genetic similarity (15-30%) [32], some sequence motives of their tertiary structures resemble each other [13] and, importantly, their co-factor binding domain is highly conserved. In humans and mouse at least 70 distinct SDR have been identified: they have a highly variable C-terminal substrate binding domain, but all contain a Rossmann-fold scaffold and bind NAD(P) dinucleotides [13, 31]. SRP-35 contains a Tyr residue with adjacent Lys and Ser residues in its active site but is slightly larger than "classical" SDR, being 311 rather than the classical 250 residues long; thus it should be classified as an "extended" member of the SDR superfamily [13]. Among the many functions catalyzed by SDR family members, some are involved in retinol/retinladehyde metabolism. Indeed, retinols (such as vitamin A) that are taken in with the diet, are transported at high concentrations via the serum, bound to retinol-

binding protein and can be taken up by any cell for storage or potential conversion to retinoic acid. Once inside the cell they are converted to retinal via a reversible reaction catalysed by SDR (or Alcohol dehydrogenases), first to retinaldehyde with the concomitant generation of NADH and subsequently to retinoic acid by cytosolic aldehyde dehydrogenases (Aldh1a1 to Aldh1a3) [34,35].

The results of the present investigation support a role for SRP-35 in the conversion of retinol to retinaldehyde and thus to its involvement in the retinoic acid signalling pathway in skeletal muscle. Skeletal muscles express RAR and high levels of RXRγ [15, 36, 37], receptors that can activate the muscle specific transcription factors myogenin and myoD [38, 39] and treatment of muscle cells in culture with retinoic acid has been shown to stimulate myotube differentiation [39, 40].

An intriguing aspect of SRP-35 is its particular tissue and subcellular distribution; in fact western blot analysis of different tissues revealed that it is abundantly expressed in liver and kidney where it is absent from the microsomal fraction but present in the post microsomal supernatant. Indeed SDRs have been found in the cytosol, in organelles such as the endoplasmic reticulum and mitochondria as well as in low density peroxisomes [41, 42], the latter being too light to be pelleted by a 1 hour centrifugation at 100'000 *g*. In order to investigate whether in liver and kidney SRP-35 is present in "light" membrane fractions, a more detailed analysis of rough and smooth ER, peroxisomes and lysosomes should be carried out. Nevertheless, in skeletal muscle SRP-35 is present in the SR and based upon our subcellular fractionation experiments, it is enriched in the longitudinal SR, a fraction also enriched in proteins such as the SERCA pump and sarcalumenin [for a recent review see ref. 11]. Such a distribution is compatible with the high resolution confocal immunofluorescence experiments of endogenous SRP-35 which revealed the presence of cross striated bands, a pattern which is similar and partially overlaps with the distribution of SERCA. We cannot exclude that in skeletal muscle targeting of SRP-35 to the longitudinal sarcoplasmic reticulum is mediated by its interaction with other proteins. Co-immunoprecipitation experiments did not reveal any interaction with either SERCA1 or SERCA2 (not shown) and binding to other SR proteins may be of low affinity and thus easily disrupted by the high salt concentration and detergents required to solubilize SRP-35. Interestingly, quantitative analysis of the content of SRP-35 in slow and fast twitch muscles indicates that this protein is enriched in fast twitch muscles; though of potential significance this may be due to the fact that the relative volume of the SR is almost double in EDL compared to soleus muscles [43-45].

The biochemical characterization of this novel muscle SDR strongly support that it is a membrane bound protein with its catalytic site facing the cytoplasm; in fact (i) it could not be extracted by treating vesicles with high salt or bicarbonate, methods which have been successfully used to extract loosely bound or soluble proteins from the ER/SR [23, 24, 46] and (ii) mild detergents such as CHAPS were not efficient at solubilising SRP-35. (iii) Trypsin digestion revealed that most of the protein faces the myoplasm; thus both its product (retinaldehyde) and NAD(P)H would be released into the myoplasm. The generation of NADH in the myoplasm may have functional signalling relevance; in fact lactate dehydrogenase requires NADH as reducing power to generate lactate from pyruvate and though NADH is available in the mitochondria where it is used to generate ATP, there are no transporters for NADH and therefore the reduced co-factor must be regenerated in the cellular compartments where it is consumed [47]. It should also be mentioned that cytosolic NADH has been shown to regulate the activity of the RyR, especially in the heart [48, 49]. Although we are aware that SRP-35 is a low abundant SR protein and we do not exactly know the stoichiometric ratio between SRP-35 and RyR1, we speculate the NADH generated by SRP-35 in a microdomain adjacent to SR membranes might allosterically modulate RyR1

activity. We can also not exclude the possibility that SRP-35 indirectly modulates Ca^{2+} release by affecting the level of expression of the RyR1 protein.

Our results show that over-expression of SRP-35 in C_2C_{12} myotubes results in a decrease of RyR1-mediated Ca^{2+} release, a result that could be mimicked by the addition of retinoic acid to the culture medium during differentiation. Indeed both the Ca^{2+} release induced by KCl (mimicking depolarization) as well as that induced by direct activation of RyR1 were reduced by approximately 40% with no significant change in the EC_{50} for either agonist. Such a result is reminiscent of the effect of mutations in the *RYR1* gene linked to some forms of central core disease and multiminicore disease; in fact mytubes from such patients have reduced pharmacologically evoked Ca^{2+}release, and, depending on the mutation increased or normal resting [Ca^{2+}] and/or reduced expression of RyR1 in muscle [25, 50-52]. In the case of SRP-35, the decreased Ca^{2+} release was not accompanied by a change in the resting [Ca^{2+}] nor in the Ca^{2+} present in intracellular stores suggesting that the effect was not due to a modification of Ca^{2+} fluxes across surface membranes [53] but likely due to reduced expression of components of the Ca^{2+} release units. Real time PCR on RA treated cells shows that the level of expression of the $Ca_v1.1$ was not affected but that of the RyR1 was reduced by approximately 50%. A result confirmed by immunoblotting. A similar effect of retinoic acid treatment on the expression of inositol- 1,4,5-trisphoshate receptors has been reported [54, 55] and is thought to be due to a decrease in the promoter activity in response to retinoic acid.

What is the function of SRP-35 *in vivo* and what is the physiological activator of this short chain dehydrogenase? Skeletal muscle constitutes approximately 40% of the total body mass, accounts for more than 30% of energy expenditure and is the major tissue involved in insulin-dependent glucose uptake. Metabolism is largely regulated by nuclear hormone receptors that function as regulators of transcription and it has been demonstrated that in mice retinoic acid treatment favours mobilization of body fat, increases fatty acid oxidation and decreases body weight [20, 56]. Though at the moment it is difficult to envisage what activates the enzymatic activity of SRP-35, its strategic subcellular localization in a compartment dedicated to Ca^{2+} homeostasis and the fact that during the conversion of retinol to retinaldehyde it would concomitantly generate NADH, indicates that it may be an important molecule linking Ca^{2+} mobilization and thus muscle contraction to the activation of metabolic functions. SRP-35 is a dehydrogenase and could reduce the NAD+ generated by lactate dehydrogenase during sustained muscle activity. In fact the NAD+ which is generated during glycolysis remains in the cytoplasm since the inner mitochondrial membrane lacks a specific transport system [47]. Interestingly many enzymes involved in the glycolytic pathway adhere to the sarcoplasmic reticulum membranes [21]. The reduction of NAD+ by SRP-35 is coupled to the conversion of all-trans- retinaldehyde to retinoic acid, an important activator of GLUT4 gene transcription [57] and regulator of RyR1 expression (Fig 5). Additionally a secondary effect of SRP-35 could be mediated by NADH which has been shown to regulate ryanodine receptor activity [49]. The development of an experimental model over-expressing SRP-35 in its skeletal muscle will allow us to investigate in greater detail many aspects of this novel short chain dehydrogenase ranging from metabolism to activation of transcription of specific genes.

REFERENCES

1. Saito, A., Seiler, S., Chu, A., and Fleischer S. (1984) Preparation and morphology of sarcoplasmic reticulum terminal cisternae from rabbit skeletal muscle. J. Cell. Biol. **99**, 875-885.

2. Schneider, M.F., and Chandler, W.K. (1972) Voltage dependent charge movement of skeletal muscle: a possible step in excitation-contraction coupling. Nature **242**, 244–246.
3. Melzer, W., Hermann-Frank, A., and Luttgau, H.C. (1995) The role of Ca2+ ions in excitation-contraction coupling of skeletal muscle fibres. Biochim. Biophys. Acta **1241**, 59–116.
4. Inesi, G., Canitlina, T., Yu, X., Nikic, D., Sagara, Y., and Kirtley, M.E. (1992) Long-range intramolecular linked functions in activation and inhibition of SERCA ATPases. Ann. N.Y. Acad. Sci. **671**, 32-47.
5. MacLennan, D.H. (2000) Ca2+ signaling and muscle disease. Eur. J. Biochem. **267**, 5291-5297.
6. MacLennan, D.H., Asahi, M., and Tupling, A.R. (2003) The regulation of SERCA-type pumps by phospholamban and sarcolipin. Ann. N.Y. Acad. Sci. **986**, 472–480.
7. Franzini-Armstrong, C., and Jorgensen, A.O. (1994) Structure and development of E-C coupling units in skeletal muscle. Annu. Rev. Physiol. **56**, 509–534.
8. Mitchell, R.D., Saito, A., Palade, P., and Fleischer, S. (1983) Morphology of isolated triads. J. Cell Biol. **96**, 1017–1029.
9. Rios, E., and Pizarro, G. (1991) Voltage sensor of excitation-contraction coupling in skeletal muscle. Physiol. Rev. **71**, 849–908.
10. Weisleder, N., Takeshima, H,. and Ma, J. (2008) Immuno-proteomic approach to excitation–contraction coupling in skeletal and cardiac muscle: molecular insights revealed by the mitsugumins. Cell Calcium **43**, 1–8.
11. Treves, S., Vukcevic, M, Maj, M., Thurnheer, R., Mosca, B., and Zorzato, F. (2009) Minor sarcoplasmic reticulum membrane components that modulate excitation-contraction coupling in striated muscles. J. Physiol. **587**, 3071-3079.
12. Persson, B., Kallberg, Y., Bray, J.E., Bruford, E., Dellaporta, S.L., Favia, A.D., Duarte, R.G., Jörnvall, H., Kavanagh, K.L., Kedishvili, N., Kisiela, M., Maser, E., Mindnich, R., Orchard, S., Penning, T.M., Thornton, J.M., Adamski, J., and Oppermann, U. (2009) The SDR (short-chain dehydrogenase/reductase and related enzymes) nomenclature initiative. Chem. Biol. Interact. **178**, 94-98.
13. Kavanagh, K.L., Jörnvall, H., Persson, B., and Oppermann U**.** (2008) Medium- and short-chain dehydrogenase/reductase gene and protein families: the SDR superfamily: functional and structural diversity within a family of metabolic and regulatory enzymes. Cell Mol. Life Sci. **65**, 3895-3990.
14. Theodosiou. M., Laudet. V., and Schubert, M. (2010) From carrot to clinic: an overview of the retinoic acid signaling pathway. Cell Mol. Life Sci. **67**, 1423-1445.
15. Mangelsdorf D.J., Borgmeyer U., Heyman R.A., Zhou J.Y., Ong E.S., Oro A.E., Kakizuka A., and Evans R.M. (1992) Characterization of three RXR genes that mediate the action of 9-cis retinoic acid. Genes Dev. **6**, 329-344.
16. Petkovich, M., Brand N.J., Krust A., and Chambon P. (1987) A human retinoic acid receptor which belongs to the family of nuclear receptors. Nature **330**, 444- 450.
17. Germain, P., Chambon, P., Eichele, G., Evans, R.M., Lazar, M.A., Leid, M., De Lera, A.R., Lotan, R., Mangelsdorf, D.J., and Groenmeyer, H. (2006) International Union of Pharmacology. LX. Retinoic acid receptors. Pharmacol. Rev. **58**, 712–725.
18. Ziouzenkova, O., and Plutzky, J. (2008) Retinoid metabolism and nuclear receptor responses: New insights into coordinated regulation of the PPAR–RXR complex. FEBS Lett. **582**, 32-38.
19. Napoli, J.L. (1996) Biochemical pathways of retinoid transport, metabolism and signal transduction. Clin. Immunol. Immunopathol **80**, S52-S62.

20. Amengual, J., Ribot, J., Bonet, M.L., and Palou, A. (2008) Retinoic acid treatment increases lipid oxidation capacity in skeletal muscle of mice. Obesity **16**, 585-591.
21. Xu, K.Y., and Becker, L.C. (1998) Ultrastructural localization of glycolytic enzymes on sarcoplasmic reticulum vesicles. J. Histochem. Cytochem. **46**, 419-427.
22. Journet, A., Chapel, A., Kieffer, S., Louwagie, M., Luche, S., and Garin, J. (2000) Towards a human repertoire of monocytic lysosomal proteins. Electrophoresis **21**, 3411-3419.
23. Anderson, A.A., Treves, S., Biral, D., Betto, R., Sandonà, D., Ronjat, M., and Zorzato, F. (2003) The novel skeletal muscle sarcoplasmic reticulum JP-45 protein. Molecular cloning, tissue distribution, developmental expression, and interaction with alpha 1.1 subunit of the voltage-gated calcium channel. J. Biol. Chem. **278**, 39987-39992.
24. Treves, S., Feriotto, G., Moccagatta, L., Gambari, R., and Zorzato, F. (2000) Molecular cloning, expression, functional characterization, chromosomal localization, and gene structure of junctate, a novel integral calcium binding protein of sarco(endo)plasmic reticulum membrane. J. Biol. Chem. **275**, 39555-39568.
25. Zorzato, F., Anderson, A.A., Ohlendieck, K., Froemming G., Guerrini, R., and Treves, S. (2000) Identification of a novel 45 kDa protein (JP-45) from rabbit sarcoplasmic-reticulum junctional-face membrane. Biochem. J. **351**, 537-543
26. Sharkis, D.H., and Swenson, R.P. (1989) Purification by cibacron blue F3GA dye affinity chromatography and comparison of NAD(P)H: quinone reductase (E.C.1.6.99.2) from rat liver cytosol and microsomes. Biochem. Biophys. Res. Commun. **161**, 434-441.
27. Ducreux. S., Zorzato, F., Müller, C., Sewry, C., Muntoni, F., Quinlivan, R., Restagno, G., Girard, T., and Treves S. (2004) Effect of ryanodine receptor mutations on interleukin-6 release and intracellular calcium homeostasis in human myotubes from malignant hyperthermia-susceptible individuals and patients affected by central core disease. J. Biol. Chem. **279**, 43838-43846.
28. Gough, W.H., VanOoteghem, S., Sint, T., and Kedishvill, N.Y. (1998) cDNA clonino and characterization of a new human microsomal NAD+-dependent dehydrogenase that oxidizes all-trans-retinol and 3 alpha-hydroxysteroids. J. Biol. Chem. **273**, 19778-19785.
29. Treves, S., Vukcevic, M., Jeannet, P.Y., Levano, S., Girard, T., Urwyler, A., Fischer, D., Voit, T., Jungbluth, H., Lillis, S., Muntoni, F., Quinlivan, R., Sarkozy, A., Bushby, K., and Zorzato, F. (2011) Enhanced excitation coupled Ca2+ entry induces nuclear translocation of NFAT and contributes to IL-6 release from myotubes from patients with Central core disease. Hum. Mol. Genetics **20**, 589-600.
30. Takeshima, H., Komazaki, S., Nishi, M., Iino, M., and Kangawa, K. (2002) Junctophilins: a novel family of junctional membrane complex proteins. Mol. Cell **6**, 11-22.
31. Persson, B., Krook, M., and Jörnvall, H. (1991) Characteristics of short-chain alcohol dehydrogenases and related enzymes. Eur. J. Biochem. **200**, 537-543.
32. Kallberg, Y., Oppermann, U., Jörnvall, H., and Persson B. (2002) Short-chain dehydrogenase/reductase (SDR) relationships: a large family with eight clusters common to human, animal, and plant genomes. Protein Sci. **11**, 636-641.
33. Persson, B., Kallberg, Y., Oppermann, U., and Jörnvall, H. (2003) Coenzyme-based functional assignments of short-chain dehydrogenases/reductases (SDRs). Chem. Biol. Interact. **143**, 271-278.
34. Duester, G. (1996) Involvement of alcohol dehydrogenase, short-chain dehydrogenase/reductase, aldehyde dehydrogenase, and cytochrome P450 in the

control of retinoid signaling by activation of retinoic acid synthesis. Biochemistry **35**, 12221-12227.
35. Parés, X., Farrés, J., Kedishvili, N., and Duester, G. (2009) Medium- and short-chain dehydrogenase/reductase gene and protein families: the SDR superfamily: functional and structural diversity within a family of metabolic and regulatory enzymes. Cell Mol. Life Sci. **65**, 3895-3906.
36. Liu, Q., and Linney, E. (1993) The mouse retinoid-X receptor-gamma gene: genomc organization and evidence for functional isoforms. Mol. Endocrinol. **7**, 651-658.
37. Smith, A.G., and Muscat G.E.O. (2005) Skeletal muscle and nuclear hormone receptors: implications for cardiovascular and metabolic disease. Int. J. Biochem. Cell Biol. **37**, 2047-2063.
38. Muscat G.E, Mynett-Johnson L., Dowhan D., Downes, M., and Griggs, R. (1994) Activation of myoD gene transcription by 3,5,3'-triodo-L-thyronine: a direct role for the thyroid hormone and retinoid X receptors. Nucleic Acids Res. **22**, 583-591.
39. Halevy, O., and Lerman, O. (1993) Retinoic acid induces adult muscle cell differentiation mediated by the retinoic acid receptor alpha. J. Cell Physiol. **154**, 566-572.
40. Zhu, G.H., Huang, J., Bi, Y., Su, Y., Tang, Y., He, B.C., He, Y., Luo, J., Wang, Y., Chen, L., Zuo, G.W., Jiang, W., Luo, Q., Shen, J., Liu, B., Zhang, W.L., Shi, Q., Zhang, B.Q., Kang, Q., Zhu, J., Tian, J., Luu, H.H., Haydon, R.C., Chen, Y., and He, T.C. (2009) Activation of RXR and RAR signaling promotes myogenic differentiation of myoblastic C2C12 cells. Differentiation **78**, 195-204.
41. Filling, C., Wu, X., Shafqat, N., Hult, M., Martensson, E., Shafqat, J., and Oppermann, U.C.T. (2001) Subcellular targeting analysis of SDR-type hydroxysteroid dehydrogenases. Mol. Cell Endocrinol. **171**, 99-101.
42. Markus, M., Husen, B., and Adamski, J. (1995) The subcellular localization of 17ß-hydroxysteroid dehydrogenase type 4 and its interaction with actin. J. Steroid Biochem. Molec. Biol. **55**, 617-621.
43. Luff, A.R., and Atwood, H.L. (1971) Changes in the sarcoplasmic reticulum and transverse tubular system of fast and slow skeletal muscles of the mouse during postnatal development. J. Cell Biol. **51**, 369-383.
44. Eisenberg, B. R., Kuda, A.M., and Peter, J.B. (1974) Stereological analysis of mammalian skeletal muscle. I. Soleus muscle of the adult guinea pig. J. Cell Biol. **60,** 732-754.
45. Franzini-Armstrong, C., and Peachey, L.D. (1981) Striated muscle contractile and control mechanisms. J. Cell Biol. **91**, 166-186.
46. Cala, S.E., and Jones, L.R. (1983) Rapid purification of calsequestrin from cardiac and skeletal muscle sarcoplasmic reticulum vesicles by Ca2+-dependent elution from phenyl-sepharose. J. Biol. Chem. **258**, 11932-11936.
47. Voet, D., and Voet, J.G. (2004). Biochemistry (ed. J. Wiley & Sons, Inc) pp 800- 802.
48. Cherednichenko G., Zima, Av.V., Feng, W., Schafer S., Blatter, L.A., and Pessah, I.N. (2004) NADH oxidase activity of rat cardiac sarcoplasmic reticulum regulates calcium induced calcium-release. Cir. Res. **94**, 478-486.
49. Zima A.V., Copello J.A., and Blatter, L.A. (2003) Differential modulation of cardiac and skeletal muscle ryanodine receptors by NADH. FEBS. Lett. **547**, 32-36.
50. Zhou, H., Yamaguchi, N., Xu, L., Wang, Y., Sewry, C., Jungbluth, H., Zorzato, F., Bertini, E., Muntoni, F., Meissner, G., and Treves S. (2006) Chracterization of recessive RYR1 mutations in core myopathies. Hum. Mol. Genet. **15**, 2791-2803.
51. Zhou, H., Jungbluth, H., Sewry, C.A., Feng, L., Bertini, E., Bushby, K., Straub, V., Roper, H., Rose, M.R., Brockington, M., Kinali, M., Manzur, A., Robb, S., Appleton,

R., Messina, S., D'Amico, A., Quinlivan, R., Swash, M., Müller, C.R., Brown, S., Treves, S., and Muntoni F. (2007) Molecular mechanisms and phenotypic variation in RYR1 related congenital myopathies. Brain. **130**, 2024-2036.
52. Ghassemi, F., Vukcevic, M., Xu, L., Zhou, H., Meissner, G., Muntoni, F., Jungbluth, H., Zorzato, F., and Treves S. (2009) A recessive ryanodine receptor 1 mutation in a CCD patient increases channel activity. Cell Calcium **45**, 192-197.
53. Rios, E. (2010) The cell boundary theorem: a simple law of the control of cytosolic calcium concentration. J. Physiol. Sci. **60**, 81-84.
54. Stefanik P., Macejova, D., Mravec, B., Brtko, J., and Krizanova, O. (2005) Distinct modulation of a gene expression of the type 1 and 2 IP3 receptors by retinoic acid in brain areas. Neurochem. Int. **46**, 559-564.
55. Deelman, L.E., Jonk, L.J.C., and Henning, R.H. (1998) The isolation and characterization of the promoter of the human type I inositol 1,4,5-trisphosphate receptor. Gene **207**, 219-225.
56. Haugen, B. Jensen, D.R., Sharma, V., Pulawa, L.K., Hays, W.R., Krezel, W., Chambon, P., and Eckel, R.H. (2004) Retinoid X receptor gamma-deficient mice have increased skeletal muscle lipoprotein lipase activity and less weight gain when fed a high-fat diet. Endocrinology **145**, 3679-3685.
57. Sleeman, M.W., Zhou, H., Rogers, S., Ng, K.W., and Best, J.D. (1995) Retinoic acid stimulates glucose transporter expression in L6 muscle cells. Mol. Cell. Endocrinol. **27**, 161-167.

FOOTNOTES

Abbreviations: CHAPS, 3-[(3-Cholamidopropyl)dimethylammonio]-1-propanesulfonate; DDM, n-dodecyl-beta-D-maltoside; DHPC, 1,2-diheptanoyl-*sn*-Glycero-3-phosphocholine; DHPR, dihydropyridine receptor; LSR, longitudinal sarcoplasmic reticulum; RA, retinoic acid; RAL, all-*trans* retinaldehyde; RAR, retinoic acid receptor; ROL, all-*trans* retinol; RXR, retinoid X receptor; RyR, ryanodine receptor; SDR, short chain dehydrogenase; SERCA, sarco(endo)plasmic reticulum CaATPase; SR, sarcoplasmic reticulum.

ACKNOWLEDGEMENTS

This work was supported by the Department of Anesthesia Basel University Hospital and grants from the Association Française contre les Myopathies, Telethon GGP08020, Ministero della Ricerca Scientifica e Tecnologica ex 40% e 60%. We would like to thank Ms Anne-Sylvie Monnet for her expert technical assistance and Caroline Steiblin for her help with the bioinformatics.

FIGURE LEGENDS

Figure 1. Predicted primary sequence of mouse SRP-35 and comparison with that of other vertebrates. Dark grey box indicates hydrophobic residues encoding the putative transmembrane domain. The two light grey boxes indicate the peptide sequences obtained from rabbit skeletal muscle SRP-35 from which primers were designed. Underlined residues indicate catalytic consensus sequence and the bold letters indicate perfectly conserved residues within the NAD(P)(H)-binding site.

Figure 2. Tissue and subcellular distribution of SRP-35. A. Total homogenates (30 µg/lane) from the indicated mouse tissues were separated on a 12.5% SDS-PAG, blotted onto nitrocellulose and probed with anti-SRP-35 Ab. **B.** Total liver homogenate, the microsomal fraction (100,000 *g* pellet) or post microsomal supernatant (100,000 *g* sup) (30 µg/lane) were loaded on a 12.5% SDS-PAG, blotted onto nitrocellulose and probed anti-SRP-35 Ab. **C.** Total SR from mouse skeletal muscle or the microsomal fraction from the indicated tissues (50 µg/lane) were separated on a 10% SDS-PAG, blotted onto nitrocellulose and probed with anti-SRP-35 antibody. **D.** Total mouse SR was fractionated into light (PM), longitudinal sarcoplasmice reticulum (LSR) and terminal cisternae (TC) (30 µg/lane); proteins were separated on a 10% SDS PAG, blotted onto nitrocellulose and probed with anti-SRP-35 Abs. **E.** C_2C_{12} myotubes transfected with the plasmid encoding pEGFP were visualized by brightfield (left) or under fluorescent light with a 20x water-immersion FLUAR objective (0.75 numerical aperture). **F.** C_2C_{12} myotubes transfected with the plasmid encoding SRP-35-EGFP were visualized by brightfield (left) or under fluorescent light. Note that in these cells fluorescence is punctuated and excluded from the nuclei (bar indicates 50 µm). **G**. Longitudinal sections of mouse skeletal muscle were stained with anti-SRP-35 followed by anti-rabbit conjugated Alexa-Fluor 488. Muscle tissue was visualized with a Leica DM1400 Confocal microscope equipped with a HCX APO 100x oil immersion TIRF objective (1.47 N.A.). Images (1024x1024) were acquired at 400 Hz through a 1 µm pinhole; note the striated distribution of SRP-35 compatible with a membrane localization. Bar indicates 10 µm. **H**. Total homogenates (20 and 40 µg) of fast (EDL) and slow (soleus) muscles were loaded on a 10% SDS PAG, the proteins were blotted onto nitrocellulose and probed with anti-SRP-35 Abs as described above. Immunoreactivity with albumin was used as a control to show that similar amounts of proteins were loaded.

Figure 3 SRP-35 is tightly associated with sarcoplasmic reticulum membranes and the majority of the protein faces the myoplasm. Total mouse SR microsomes were incubated for 30 min on ice with either **(A)** KCl or **(B)** Na_2CO_3 and centrifuged at 150,000 *g* for 45 min. Proteins present in the supernatant and in the pellet were separated on a 12.5 % SDS-PAGE and stained with anti-SRP-35 antibodies or Stains-All (to visualize calsequestrin which stains metachromatically blue). **(C)** Total mouse skeletal muscle sarcoplasmic reticulum (1 mg/ml) was treated with the indicated detergent (1%) in presence of 1M NaCl for 30 min at 4°C. After centrifugation at 135,000 *g*, pellets and supernatant were collected and proteins (30 µg/lane) were separated by a 12.5 % SDS-PAGE, blotted onto nitrocellulose and stained with SRP-35 Abs. Total sarcoplasmic reticulum from mouse skeletal muscles (50 µg protein) were treated with increasing concentrations of trypsin, for 2 min at RT. After treatment, the reaction was blocked and proteins were loaded onto a 12.5% SDS-PAGE, blotted onto nitrocellulose and stained with antibodies against SRP-35 (left) and calregulin (as a control for vesicle integrity). NT: no treatment;

Figure 4 SRP-35 is a dinucleotide binding protein and its over-expression leads to an increased production of all-*trans* retinaldehyde. SRP-35 binds Cibacron Blue F3G-A a ligand. **A**: 1 mg/ml total SR vescicles were solubilized in a solution containing 1% DDM, 1M NaCl and subsequently incubated with Cibacron Blue F3G-A resin as described in the Methods section. Proteins present in the total SR (30 μg, lanes 1), pellet after solubilization with DDM/NaCl (30 μl lane 2), total SR proteins solubilized with DDM/NaCl (30 μl, lane 3), void (30 μl, lane 4), last wash (30 μl, lane 5), eluted with NADH (30 μl, lanes 6) and attached to the resin (30 μl, lanes 7). Left panel, Ponceau Red stained blot; right panel, blot stained with anti-SRP-35 Abs. **B** as A, except that blot was stained with anti-calsequestin antibodies. Note that calsequestrin does not bind to Cibacron Blue F3G-A. **C** and **D**: Chromograms (325 nm) of the homogenates of pEYFPC1 and pEYFPC1-SRP-35 transfected HEK293 cells. All-*trans* retinylester (1), all-*trans* retinaldehyde-oxim (syn: 2; anti: 5) (RAL), 13-cis retinol (3) and all-*trans* retinol (4) (ROL). The peaks are identified by authentic standards. **E** and **F**: Bar histograms comparing the percentage of Retinaldehyde and Retinol present in pEYFPC1 and pEYFPC1-SRP-35 transfected cells. Results are the mean (± SEM) of the experiments. The percentage of RAL in cells over-expressing SRP-35 was significantly higher than in YFP-transfected cells, $P<0.019$.

Figure 5 Effect of SRP-35 on calcium fluxes in C_2C_{12} myotubes. A and **B**: KCl- and 4-chloro-m-cresol dose response curves in C_2C_{12} transfected with pEYFPC1 (full line) or pEYFPC1-SRP-35 (dashed line). Data points represent the mean peak fluorescence increase of 6-11 cells. Curves were fit using a Boltzmann equation; there were no significant differences in the EC_{50} for KCl or 4-chloro-m-cresol. **C**: SRP-35 over-expression does not affect the resting $[Ca^{2+}]$ of C_2C_{12} cells. **D** and **E**: Peak fura-2 Δ fluorescence (mean ± SEM of the indicated number of cells) in C_2C_{12} transfected with pEYFPC1 (empty bars), pEYFPC1-SRP-35 (dark grey bars), untreated (empty bars) and treated with retinoic acid (5 μM) for 4 days. * $P<0.005$; ** $P<0.01$; *** $P<0.008$. **F, G** and **H**: real time RT-PCR on control or RA treated C_2C_{12} cells. RA does not affect the relative expression level of $Ca_V1.1$, but it significantly increases the relative expression level of SRP-35 while decreasing that of RyR1. Results are expressed as mean± SEM of the indicated number of experiments. *** $P< 0.001$.

Figure 1

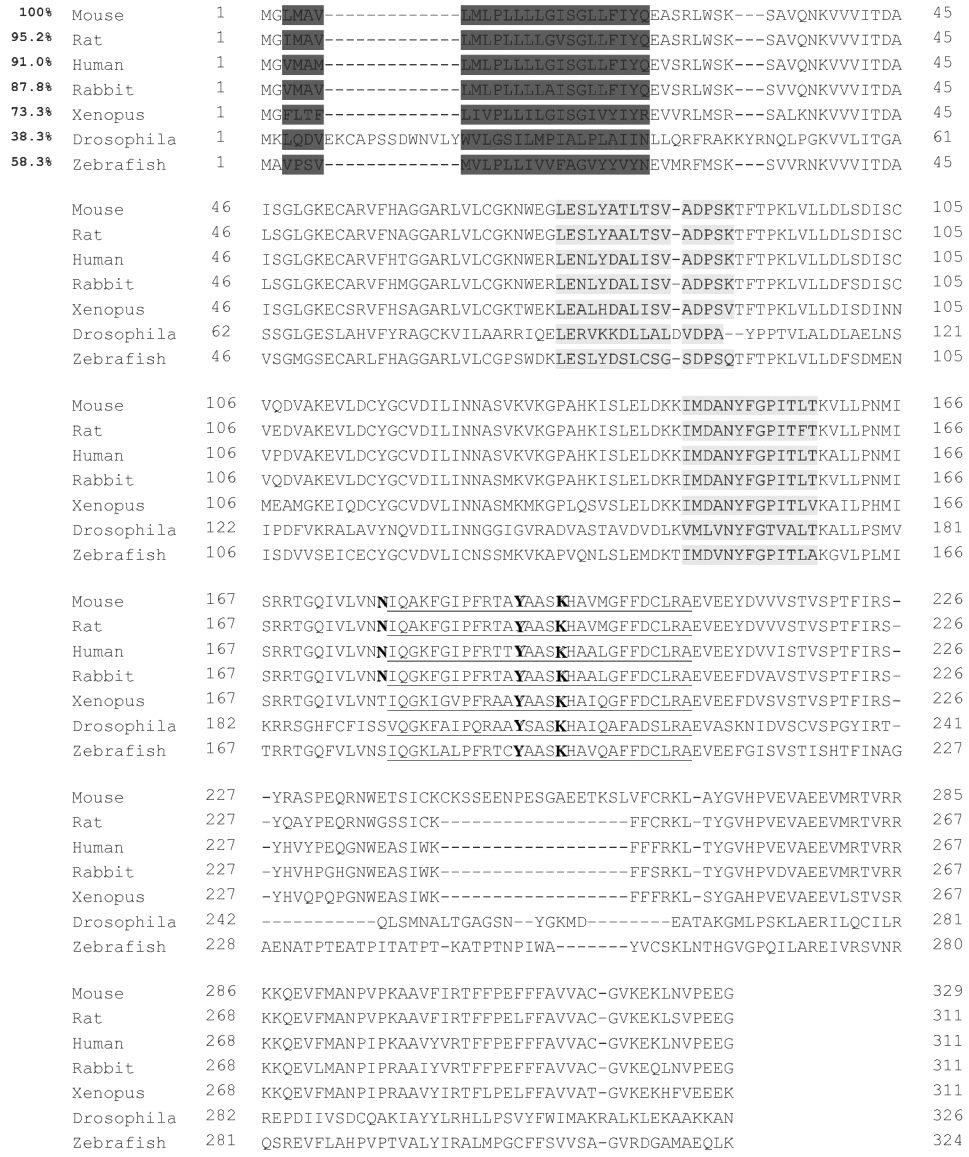
100% Mouse 1 MGLMAV----------LMLPLLLLGISGLLFIYQEASRLWSK---SAVQNKVVVITDA 45
95.2% Rat 1 MGTMAV----------LMLPLLLLGVSGLLFIYQEASRLWSK---SAVQNKVVVITDA 45
91.0% Human 1 MGVMAM----------LMLPLLLLGISGLLFIYQEVSRLWSK---SAVQNKVVVITDA 45
87.8% Rabbit 1 MGVMAV----------LMLPLLLLAISGLLFIYQEVSRLWSK---SVVQNKVVVITDA 45
73.3% Xenopus 1 MGPLTF----------LIVPLLILGISGIVYIYREVVRLMSR---SALKNKVVVITDA 45
38.3% Drosophila 1 MKLQDVEKCAPSSDWNVLYWVLGSILMPIALPLAIINLLQRFRAKKYRNQLPGKVVLITGA 61
58.3% Zebrafish 1 MAVPSV----------MVLPLLIVVFAGVYYVYNEVMRFMSK---SVVRNKVVVITDA 45
Mouse 46 ISGLGKECARVFHAGGARLVLCGKNWEGLESLYATLTSV-ADPSKTFTPKLVLLDLSDISC 105
Rat 46 LSGLGKECARVFNAGGARLVLCGKNWEGLESLYAALTSV-ADPSKTFTPKLVLLDLSDISC 105
Human 46 ISGLGKECARVFHTGGARLVLCGKNWERLENLYDALISV-ADPSKTFTPKLVLLDLSDISC 105
Rabbit 46 LSGLGKECARVFHMGGARLVLCGKNWERLENLYDALISV-ADPSKTFTPKLVLLDFSDISC 105
Xenopus 46 ISGLGKECSRVFHSAGARLVLCGKTWEKLEALHDALISV-ADPSVTFTPKLVLLDISDINN 105
Drosophila 62 SSGLGESLAHVFYRAGCKVILAARRIQELERVKKDLLALDVDPA--YPPTVLALDLAELNS 121
Zebrafish 46 VSGMGSECARLFHAGGARLVLCGPSWDKLESLYDSLCSG-SDPSQTFTPKLVLLDFSDMEN 105
Mouse 106 VQDVAKEVLDCYGCVDILINNASVKVKGPAHKISLELDKKIMDANYFGPITLTKVLLPNMI 166
Rat 106 VEDVAKEVLDCYGCVDILINNASVKVKGPAHKISLELDKKIMDANYFGPITFTKVLLPNMI 166
Human 106 VPDVAKEVLDCYGCVDILINNASVKVKGPAHKISLELDKKIMDANYFGPITLTKALLPNMI 166
Rabbit 106 VQDVAKEVLDCYGCVDILINNASMKVKGPAHKISLELDKRIMDANYFGPITLTKVLLPNMI 166
Xenopus 106 MEAMGKEIQDCYGCVDVLINNASMKMKGPLQSVSLELDKKIMDANYFGPITLVKAILPHMI 166
Drosophila 122 IPDFVKRALAVYNQVDILINNGGIGVRADVASTAVDVDLKVMLVNYFGTVALTKALLPSMV 181
Zebrafish 106 ISDVVSEICECYGCVDVLICNSSMKVKAPVQNLSLEMDKTIMDVNYFGPITLAKGVLPLMI 166
Mouse 167 SRRTGQIVLVNNIQAKFGIPFRTAYAASKHAVMGFFDCLRAEVEEYDVVVSTVSPTFIRS- 226
Rat 167 SRRTGQIVLVNNIQAKFGIPFRTAYAASKHAVMGFFDCLRAEVEEYDVVVSTVSPTFIRS- 226
Human 167 SRRTGQIVLVNNIQGKFGIPFRTTYAASKHAALGFFDCLRAEVEEYDVVISTVSPTFIRS- 226
Rabbit 167 SRRTGQIVLVNNIQGKFGIPFRTAYAASKHAALGFFDCLRAEVEEFDVAVSTVSPTFIRS- 226
Xenopus 167 SRRTGQIVLVNTIQGKIGVPFRAAYAASKHAIQGFFDCLRAEVEEFDVSVSTVSPTFIRS- 226
Drosophila 182 KRRSGHFCFISSVQGKFAIPQRAAYSASKHAIQAFADSLRAEVASKNIDVSCVSPGYIRT- 241
Zebrafish 167 TRRTGQFVLVNSIQGKLALPFRTCYAASKHAVQAFFDCLRAEVEEFGISVSTISHTFINAG 227
Mouse 227 -YRASPEQRNWETSICKCKSSEENPESGAEETKSLVFCRKL-AYGVHPVEVAEEVMRTVRR 285
Rat 227 -YQAYPEQRNWGSSICK----------FFCRKL-TYGVHPVEVAEEVMRTVRR 267
Human 227 -YHVYPEQGNWEASIWK----------FFFRKL-TYGVHPVEVAEEVMRTVRR 267
Rabbit 227 -YHVHPGHGNWEASIWK----------FFSRKL-TYGVHPVDVAEEVMRTVRR 267
Xenopus 227 -YHVQPQPGNWEASIWK----------FFFRKL-SYGAHPVEVAEEVLSTVSR 267
Drosophila 242 ----------QLSMNALTGAGSN--YGKMD--------EATAKGMLPSKLAERILQCILR 281
Zebrafish 228 AENATPTEATPITATPT-KATPTNPIWA-------YVCSKLNTHGVGPQILAREIVRSVNR 280
Mouse 286 KKQEVFMANPVPKAAVFIRTFFPEFFFAVVAC-GVKEKLNVPEEG 329
Rat 268 KKQEVFMANPVPKAAVFIRTFFPELFFAVVAC-GVKEKLSVPEEG 311
Human 268 KKQEVFMANPIPKAAVYVRTFFPEFFFAVVAC-GVKEKLNVPEEG 311
Rabbit 268 KKQEVLMANPIPRAAIYVRTFFPEFFFAVVAC-GVKEQLNVPEEG 311
Xenopus 268 KKQEVFMANPIPRAAVYIRTFLPELFFAVVAT-GVKEKHFVEEEK 311
Drosophila 282 REPDIIVSDCQAKIAYYLRHLLPSVYFWIMAKRALKLEKAAKKAN 326
Zebrafish 281 QSREVFLAHPVPTVALYIRALMPGCFFSVVSA-GVRDGAMAEQLK 324

Figure 2

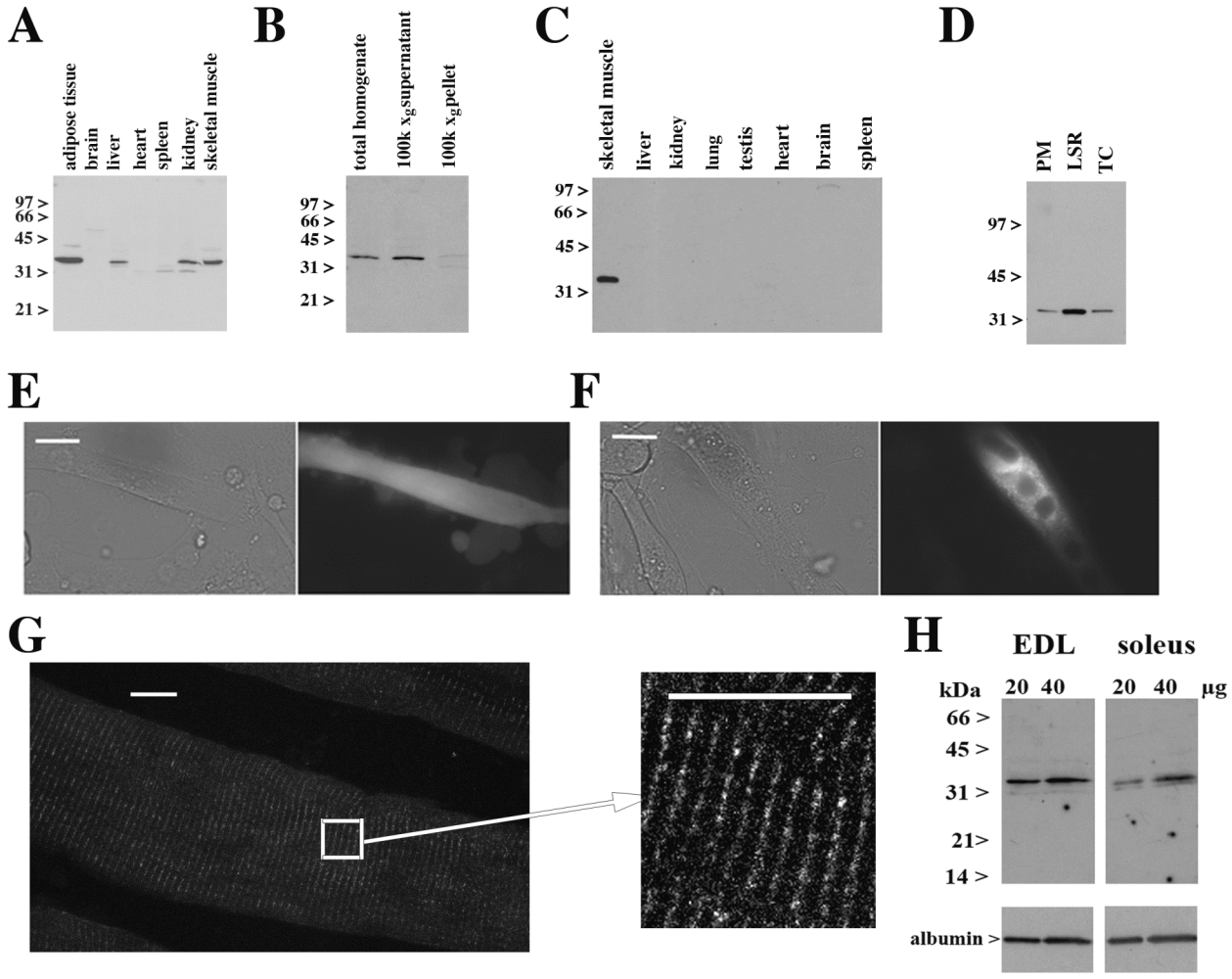
A
adipose tissue
brain
liver
heart
spleen
kidney
skeletal muscle
97 >
66 >
45 >
31 >
21 >
B
total homogenate
100k xgsupernatant
100k xgpellet
97 >
66 >
45 >
31 >
21 >
C
skeletal muscle
liver
kidney
lung
testis
heart
brain
spleen
97 >
66 >
45 >
31 >
D
PM
LSR
TC
97 >
45 >
31 >
E
F
G
H
EDL
soleus
kDa
20 40
20 40
µg
66 >
45 >
31 >
21>
14 >
albumin >

Figure 3

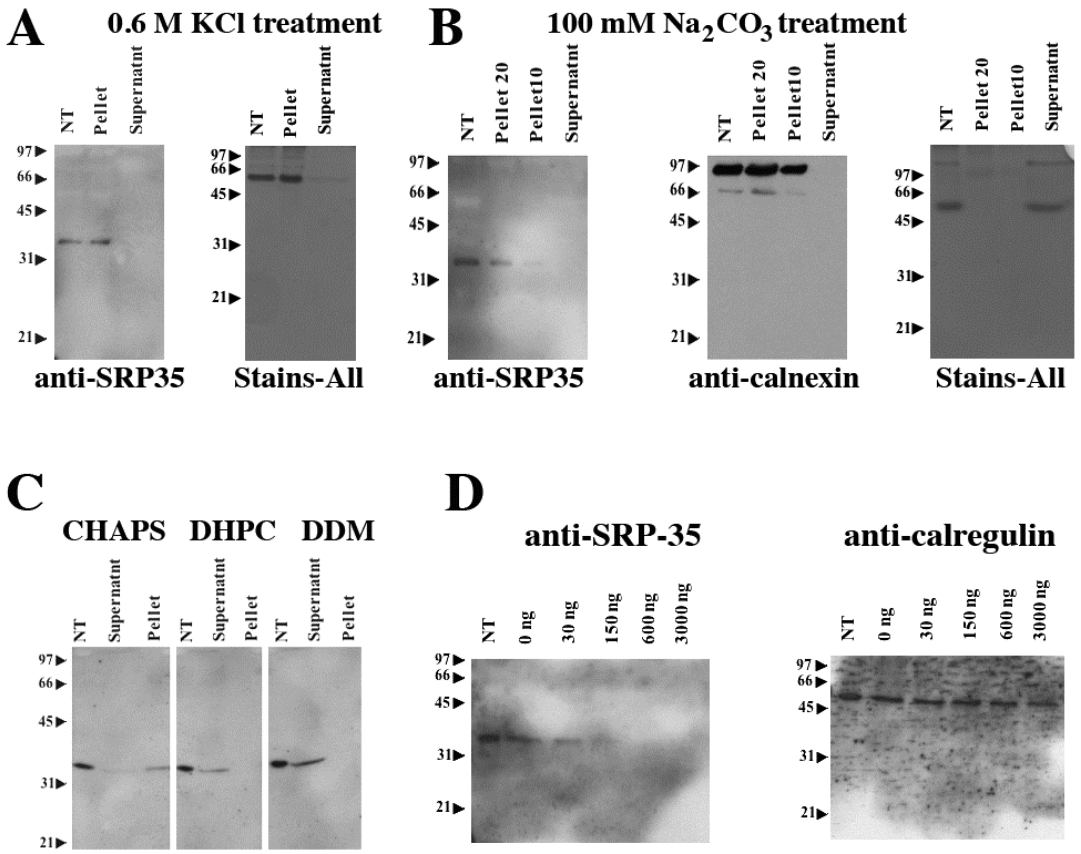
A
0.6 M KCl treatment
NT
Pellet
Supernatnt
97
66
45
31
21
anti-SRP35
Stains-All
B
100 mM Na2CO3 treatment
Pellet 20
Pellet10
anti-SRP35
anti-calnexin
C
CHAPS
DHPC
DDM
D
anti-SRP-35
anti-calregulin
0 ng
30 ng
150 ng
600 ng
3000 ng

Figure 4

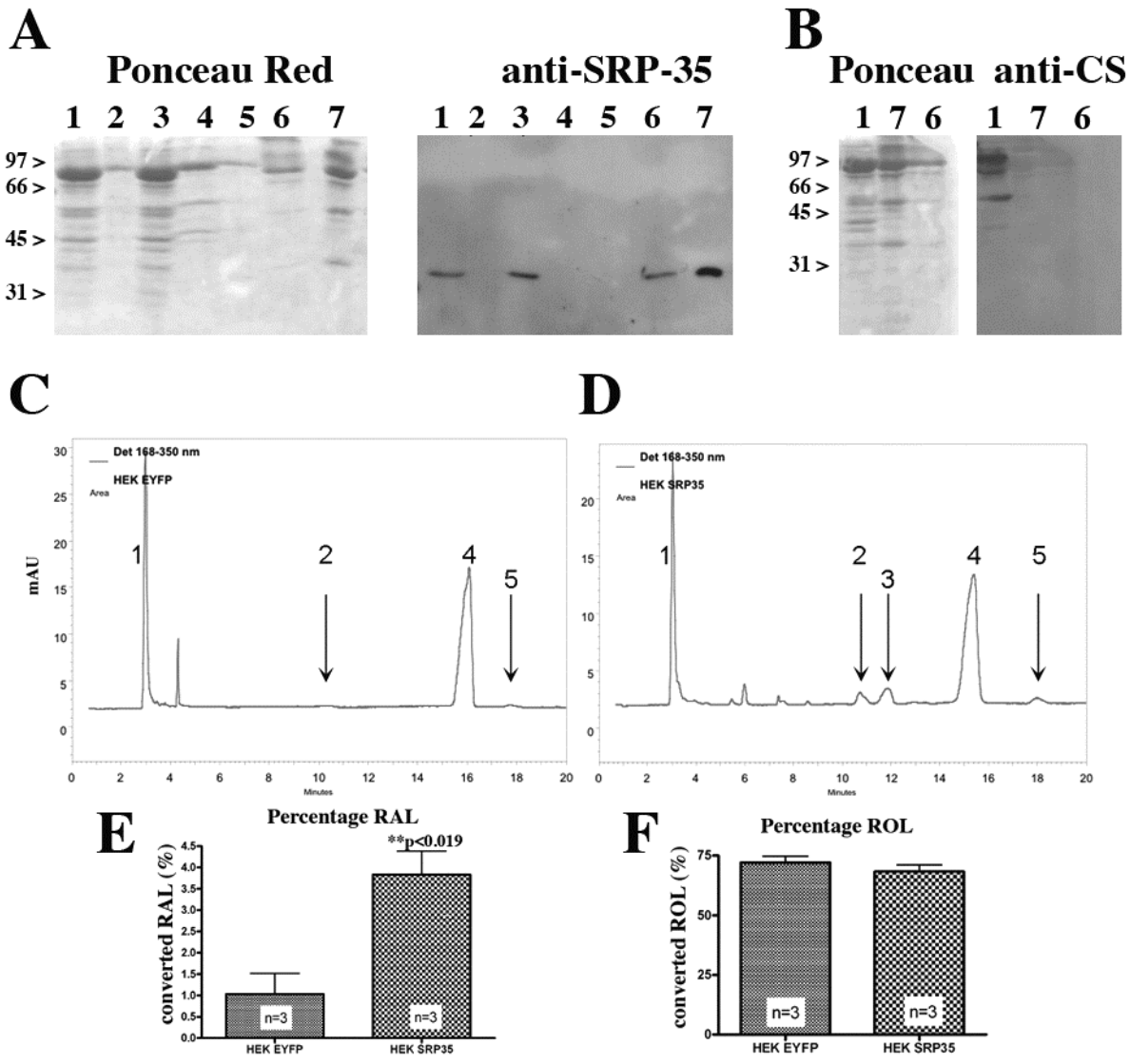
A
Ponceau Red
anti-SRP-35
1 2 3 4 5 6 7
97 >
66 >
45 >
31 >
B
Ponceau anti-CS
1 7 6 1 7 6
C
D
Det 168-350 nm
HEK EYFP
HEK SRP35
mAU
Minutes
E
Percentage RAL
**p<0.019
converted RAL (%)
n=3
HEK EYFP
HEK SRP35
F
Percentage ROL
converted ROL (%)

Figure 5

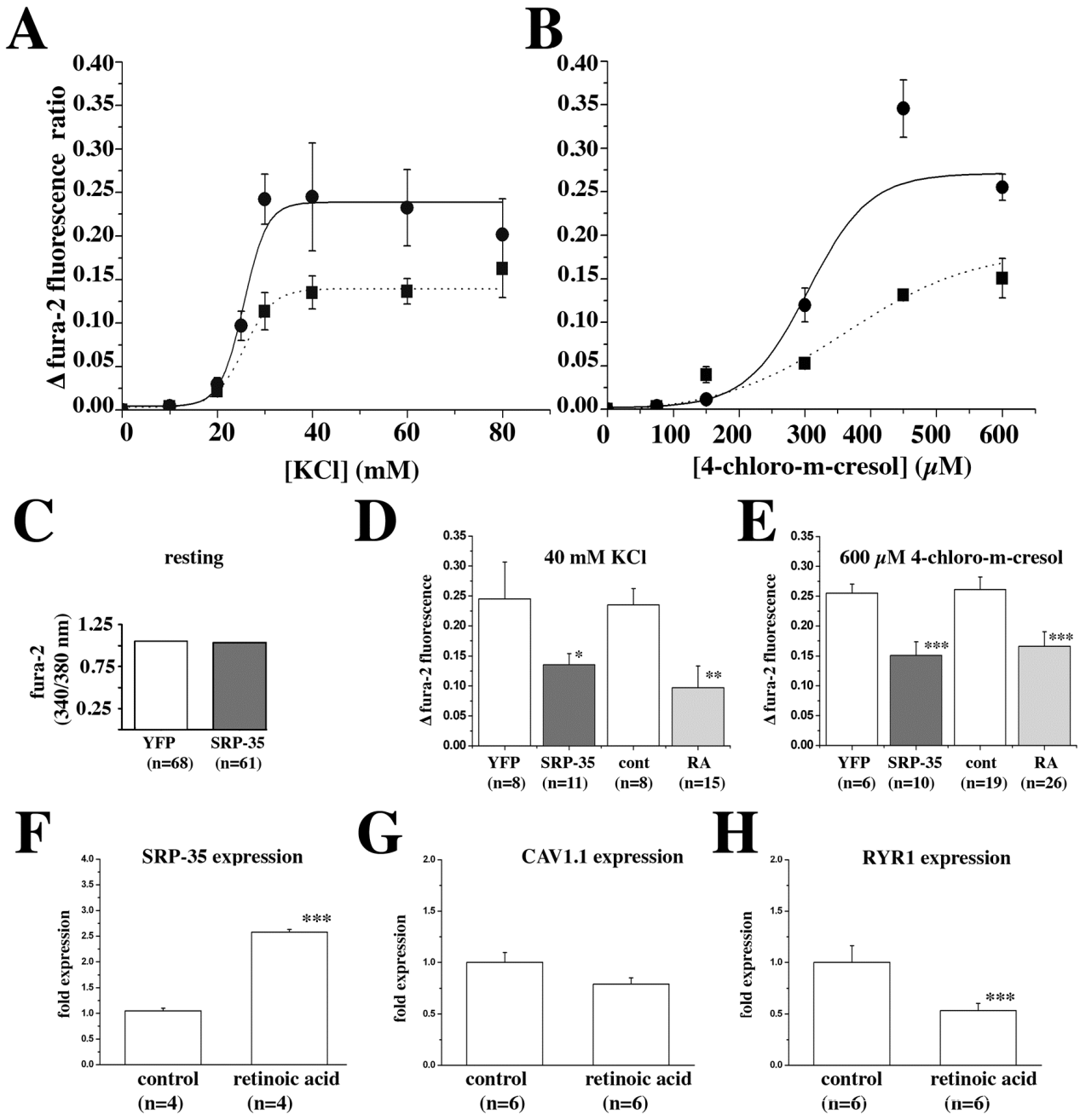
A
Δ fura-2 fluorescence ratio
0.40
0.35
0.30
0.25
0.20
0.15
0.10
0.05
0.00
0
20
40
60
80
[KCl] (mM)
B
0.40
0.35
0.30
0.25
0.20
0.15
0.10
0.05
0.00
0
100
200
300
400
500
600
[4-chloro-m-cresol] (μM)
C
resting
fura-2 (340/380 nm)
1.25
0.75
0.25
YFP (n=68)
SRP-35 (n=61)
D
40 mM KCl
Δ fura-2 fluorescence
0.35
0.30
0.25
0.20
0.15
0.10
0.05
0.00
*
**
YFP (n=8)
SRP-35 (n=11)
cont (n=8)
RA (n=15)
E
600 μM 4-chloro-m-cresol
Δ fura-2 fluorescence
0.35
0.30
0.25
0.20
0.15
0.10
0.05
0.00
***
***
YFP (n=6)
SRP-35 (n=10)
cont (n=19)
RA (n=26)
F
SRP-35 expression
fold expression
4.0
3.5
3.0
2.5
2.0
1.5
1.0
0.5
0.0
***
control (n=4)
retinoic acid (n=4)
G
CAV1.1 expression
fold expression
2.0
1.5
1.0
0.5
0.0
control (n=6)
retinoic acid (n=6)
H
RYR1 expression
fold expression
2.0
1.5
1.0
0.5
0.0
***
control (n=6)
retinoic acid (n=6)